

## THERMOGRAVIMETRIC STUDY OF THE SULPHUR DIOXIDE REACTION WITH LIME

S. DRAGAN<sup>1</sup>, A. FRIEDL<sup>2</sup>, M. HARASEK<sup>2</sup>, MIHAELA DRAGAN<sup>1</sup>, and I. SIMINICEANU<sup>3</sup>

**ABSTRACT.** Experimental thermogravimetric measurements, employing a CAHN TG- 121 system, have been performed on the reaction of sulphur dioxide and oxygen with calcined limestone. The conversions versus time of calcined limestone, ranging in particle size from 25 to 900  $\mu\text{m}$ , were measured over the temperature range 973- 1173 K and a gas rate of 0.0230 to 0.0277 m/s. On the basis of experimental data, using the unreacted core model, the kinetic parameters have been identified and the kinetic regimes evaluated. Although the external mass transfer had no influence, the internal diffusion resistance could not be avoided even with the particles as small as 25  $\mu\text{m}$  in diameter.

### INTRODUCTION

Sulphur dioxide is a major pollutant of the atmosphere, whose main effect is the *acid rain* [1]. It is produced whenever fuels, particularly coal and oil containing sulphur, burn in excess oxygen. One way of minimizing emissions of  $\text{SO}_2$  is to absorb it on solid calcium oxide, produced by calcining limestone:



The porous solid CaO can then react with  $\text{SO}_2$  in the presence of oxygen to give calcium sulphate, via the reaction (2):



This process, proposed by Borgwardt thirty years ago, is also known as the *dry injection process* [2]. The limits and the potentials of the *dry injections process* were analyzed in detail by Bjerle et al. [1] by reviewing the published works. Their conclusion was rather optimistic: "the dry injection technique is really the dream process for the power plant operator because of low investment and operating cost, compared with other available choice". Maybe for this reason the process has

---

<sup>1</sup> University "Babeș-Bolyai" of Cluj-Napoca, Faculty of Chemistry and Chemical Engineering, Str. Arany Janos 11, Cluj-Napoca, Romania, e-mail: sdragan@chem.ubbcluj.ro

<sup>2</sup> Technical University of Vienna, Austria.

<sup>3</sup> Technical University of Iași, Faculty of Industrial Chemistry, 71 Bd. Mangeron, 6600 Iași, Romania, Fax: 40-32-211667, e-mail: isiminic@ch.tuiasi.ro.

been extensively studied both by scientists involved in the environmental protection [3-9] and by academics interested in solid-gas reactions [10–33]. The representative are Borgwardt for the first group, and professor Hartman from the Czech Academy, Prague, for the second. In spite of the large amount of theoretical and experimental work carried out on this process the dependence of its rate controlling mechanism upon the operating factors is still not clearly understood. The aim of the present paper is to present our thermogravimetric results and their interpretation in order to identify the rate determining step and the kinetic parameters.

## EXPERIMENTAL

The primary kinetic data of any chemical process are the conversion versus time curves. Such data have been already obtained for the lime sulphation reaction by continuous measurement of gas phase SO<sub>2</sub> concentration at the outlet of the reactor [14,15]; discontinuous gravimetric or chemical analysis of reacted particles in a fixed bed reactor [3,12,16,17]; as well as by continuous thermogravimetric analysis [18-20]. The continuous weight measurement by a recording thermobalance seems to be the most suitable because of the accuracy and reproducibility of results. The reaction (2) is accompanied by an important solid weight increase, and the effects of side reactions are negligible. On the basis of materials balance equations (3):

$$\begin{aligned}
 m_{CaO} &= m_{CaO}^0 - m_{CaO}^0 \cdot \eta_{CaO} \\
 m_{CaSO_4} &= \frac{136}{56} m_{CaO}^0 \cdot \eta_{CaO} \\
 m_{A''} &= m_{A''}^0 \\
 m_S &= m_S^0 \left( 1 + \frac{80}{56} x_{CaO} \eta_{CaO} \right)
 \end{aligned}
 \tag{3}$$

the relation between the solid mass increase ( $\Delta m_S$ ) and the fractional conversion of lime ( $\eta_{CaO}$ ) can be derived:

$$\eta_{CaO} = \frac{56}{80} \frac{\Delta m_S}{x_{CaO}^0 \cdot m_S^0}
 \tag{4}$$

According to the equation (4), at an average conversion of 50 %, a sample of 100 mg pure lime increase in weight with 71.42 mg because of sulphation reaction (2).

The experimental equipment used in our kinetic measurements was a CAHN TG-121 system (Figure 1).

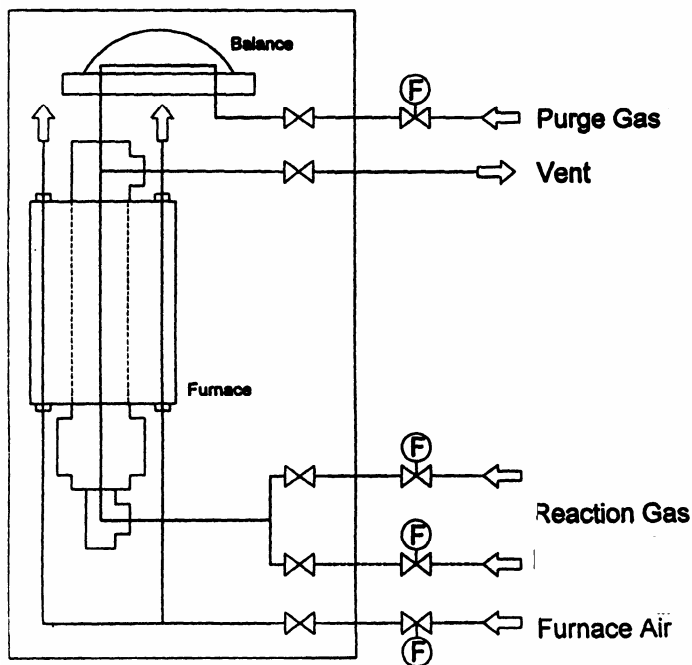


**Figure 1.** The gas circulation diagram in the main frame on the CHAN TG-121 experimental system.

It consisted of two main sections: the main frame and the Data Acquisition and Control Station (DACS) which controlled the system. The microbalance, the furnace, the cooling fan, the thermocouple, the gas and vacuum ports were the components of the main frame. The CAHN microbalance included in the TG-121 system is considered the finest apparatus available today for this application. Its sensitivity is of  $0.1 \mu\text{g}$  and the maximum capacity of 1.5 g. This balance has a closed loop servo controlled transducer which automatically compensates for weight changes in the sample. The measured weight is displayed both on the DACS monitor and on the weight display in the front panel. The furnace assures a uniform heating zone with a temperature up to 1373 K. Typically, the ramping temperature in the thermogravimetric experiments varied from  $5^\circ \text{C}/\text{min}$ . up to  $25^\circ \text{C}/\text{min}$ . The reactor, located in the furnace, had a  $125 \text{ cm}^3$  volume (22 mm diameter and 329 mm high) and was operated at a pressure of 0.3403 bar. Typical flow rates of reacting and purge gas were between 50 and  $100 \text{ cm}^3/\text{min}$ . The gas handling system provided a purge gas for the microbalance (argon), air flow for furnace cooling, and reactive pure gases from cylinders (sulfur dioxide, oxygen, and nitrogen).

Each sample of limestone has been primarily calcinated for 40 minutes at 973 K and 0.3403 bar. The thirty probes belonged to one of the following granulometric classes: 0- 50  $\mu \text{m}$ , 80 - 100  $\mu \text{m}$ , 160 -200  $\mu \text{m}$ , 400 -500  $\mu \text{m}$ , and 800 -1000  $\mu \text{m}$ .

After the complete calcination, each sample has been sulphated in a gas mixture containing 0.9 % (vol.) or 0.3 % (vol.) SO<sub>2</sub>, 20 % (vol.) O<sub>2</sub>, and nitrogen for the balance. The gas mixture was prepared from pure gases measured with rotameters.

The flow rate of the gas mixture was 50 cm<sup>3</sup>/min. in 11 of the 12 runs. The temperature in the sulphation process was kept constant at 973 K, 1023 K, 1123 K, and 1173 K respectively. The solid weight has been continuously registered, and tabulated at five minutes intervals.

## RESULTS AND DISCUSSION

The primary thermogravimetric measurements have been converted into kinetic curves with the equation (4). The conversion versus time curves for the extreme particles sizes are presented in Figures 2 and 3.

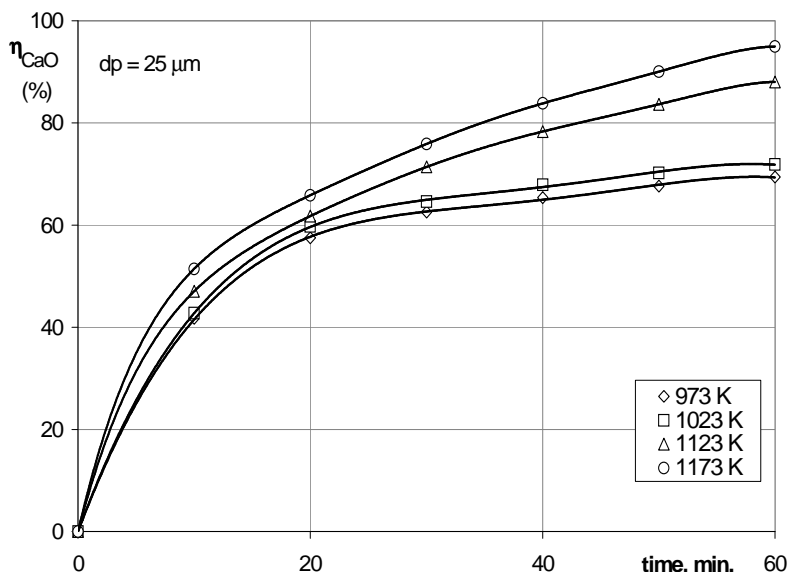


**Figure 2.** Isothermal kinetic curves, at:  $T_c = 973$  K,  $\tau_c = 40$  min.,  $P = 0.3403$  bar,  $V_g = 50$  cm<sup>3</sup>/min, % vol SO<sub>2</sub> = 0.9, and  $R_0 = 12.5$  μ m.

The experimental values of the fractional conversion of CaO illustrate the influence of two important parameters: temperature and particle size. With small particles (Figure 2) conversions above 50 % are possible in only 10 minutes, at 1173 K. The influence of temperature on the conversion of such particles, at a given time, is rather significant. This may suggest a transformation rate determining step, with a great activation energy. With large particles (Figure 3) the conversion of 50 % is not attainable even at the highest temperature and after a reaction times as long as 60 minutes. This could be due to a strong influence of the SO<sub>2</sub> diffusion through the solid product layer. The sensitivity to temperature of the conversion of

such large particles is less important, as one can see from the Figure 3. This lack of the sensitivity to temperature may be a qualitative confirmation for a mass transfer kinetic regime. Nevertheless, a more accurate and quantitatively supported interpretation of the experimental results is not possible without a postulated model describing the process.

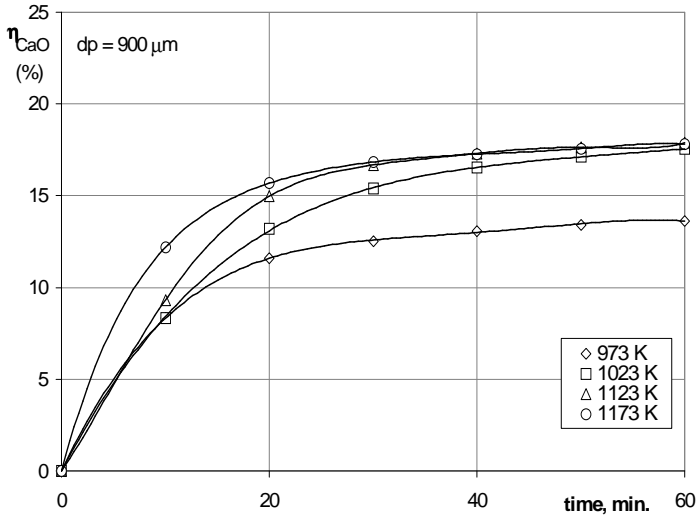


**Figure 3.** Isothermal kinetic curves at:  $T_c = 973\text{ K}$ ,  $\tau_c = 40\text{ min}$ ,  $P = 0.3403\text{ bar}$ ,  $V_g = 50\text{ cm}^3/\text{min}$ ,  $\% \text{ vol SO}_2 = 0.9$ , and  $R_0 = 450\ \mu\text{m}$

### Kinetic modeling

If the lime is considered to be made of spherical and homogeneous solid particles the *shrinking unreacted core model* may be applied for the kinetic modeling of this solid- gas process. Other improved models take into consideration the physical texture of the solid, and the intraparticle physical and chemical phenomena involved. The application of such grain or pore models needs complementary experimental data on the intraparticle surface area (BET measurements) molar volume / density of the solid product (X – ray diffraction analysis) as well as pore size distribution in particles. In the absence of such complementary data the only model to be used is the unreacted core model. This model postulates that the overall chemical process is made of three steps in series: (I) mass transfer through the gas film to the outer surface of the particle with radius  $R_0$ ; (II) the diffusion through the solid product layer; (III) the pseudo first order chemical reaction (2) at the surface of the unreacted core of radius  $R$ . The kinetic equations of the three steps are the following:

$$-\frac{dn_{SO_2}}{S_{ex} d\tau} = k_g (C_{SO_2} - C^s_{SO_2}) \quad (5)$$

$$-\frac{dn_{SO_2}}{S_r d\tau} = D_s \frac{dC_{SO_2}}{dR} \quad (6)$$

$$-\frac{dn_{SO_2}}{S_r d\tau} = kC_{SO_2} \quad (7)$$

Using the pseudo- stationarity hypothesis, the integration of these equations gives the time required to move the reaction front from the external surface of the lime particle (a sphere of radius  $R_0$ ) to the unreacted core of radius  $R$ :

$$\tau = \frac{R_0 C_{CaO}^0}{C_{SO_2}} \left[ \frac{1}{3} \left( \frac{1}{k_g} + \frac{R_0}{D_s} \right) \left( 1 - \frac{R^3}{R_0^3} \right) + \frac{R_0}{2D_s} \left( 1 - \frac{R^2}{R_0^2} \right) + \frac{1}{k} \left( 1 - \frac{R}{R_0} \right) \right] \quad (8)$$

By introducing the fractional conversion defined by (9) :

$$\eta_{CaO} = 1 - \left( \frac{R}{R_0} \right)^3 \quad (9)$$

the equation (8) becomes:

$$\tau = \frac{R_0 C_{CaO}^0}{C_{SO_2}} \left\{ \frac{1}{3k_g} \eta_{CaO} + \frac{R_0}{6D_s} \left[ 1 + 2(1 - \eta_{CaO}) - 3(1 - \eta_{CaO})^{2/3} \right] + \frac{1}{k} \left[ 1 - (1 - \eta_{CaO})^{1/3} \right] \right\} \quad (10)$$

The time required for the complete conversion of the solid particle ( $\tau^*$ ) is found by setting  $\eta_{CaO} = 1$  in the equation (10):

$$\tau^* = \frac{R_0 C_{CaO}^0}{C_{SO_2}} \left( \frac{1}{3k_g} + \frac{R_0}{6D_s} + \frac{1}{k} \right) \quad (11)$$

By combining equations (10) and (11) the kinetic model of the process can be derived in a dimensionless form:

$$\frac{\tau}{\tau^*} = \frac{\left[ \frac{1}{3k_g} \eta_{CaO} \right] + \frac{R_0}{6D_s} \left[ 1 + 2(1 - \eta_{CaO}) - 3(1 - \eta_{CaO})^{2/3} \right] + \frac{1}{k} \left[ 1 - (1 - \eta_{CaO})^{1/3} \right]}{\frac{1}{3k_g} + \frac{R_0}{6D_s} + \frac{1}{k}} \quad (12)$$

The equation (12) suggests that the three "resistances" involved are purely in series, the "overall" rate coefficient being of the form:

$$\frac{1}{K} = \frac{1}{3k_g} + \frac{R_0}{6D_s} + \frac{1}{k} \quad (13)$$

To prove its adequacy, the extreme cases also called "simple macrokinetic models", are derived from the general equation (10).

Case 1. The external mass transfer is the rate determining step (RDS), the other two resistances being negligible. ( $1/k = 0$  ;  $R_0/6D_s = 0$ ) :

$$\frac{\tau}{\tau^*} = F(\eta) = \eta_{CaO}, \text{ where } \tau^* = \frac{R_0 C_{CaO}^0}{3k_g C_{SO_2}} \quad (14)$$

Case II. The diffusion through solid product layer (CaSO<sub>4</sub>) is RDS (1/k = 0; 1/3k<sub>g</sub> = 0) and the equation (10) becomes:

$$\frac{\tau}{\tau^*} = 1 + 2(1 - \eta_{CaO}) - 3(1 - \eta_{CaO})^{\frac{2}{3}} = F(\eta), \text{ with } \tau^* = \frac{R_0^2 C_{CaO}^0}{6D_S C_{SO_2}} \quad (15)$$

Case III. When the overall process is kinetically controlled by the chemical reaction at the core surface, the two mass transfer steps being very rapid (1/3k<sub>g</sub> = 0; R<sub>0</sub>/6D<sub>S</sub> = 0) the equation (10) becomes:

$$\frac{\tau}{\tau^*} = F(\eta) = 1 - (1 - \eta_{CaO})^{\frac{1}{3}}, \text{ where } \tau^* = \frac{R_0 C_{CaO}^0}{k C_{SO_2}} \quad (16)$$

In addition to these three extreme cases and the general one (IV) described by equation (10), other three cases, with two comparable step rates, are possible: (V) external transfer and diffusion, (VI) diffusion and reaction, (VII) external transfer and reaction. Which one of these seven kinetic regimes is the most advantageous for practice? By numerical solution of the equation (12), for five frequently encountered kinetic regimes, the simulated curves in Figure 4 have been generated.

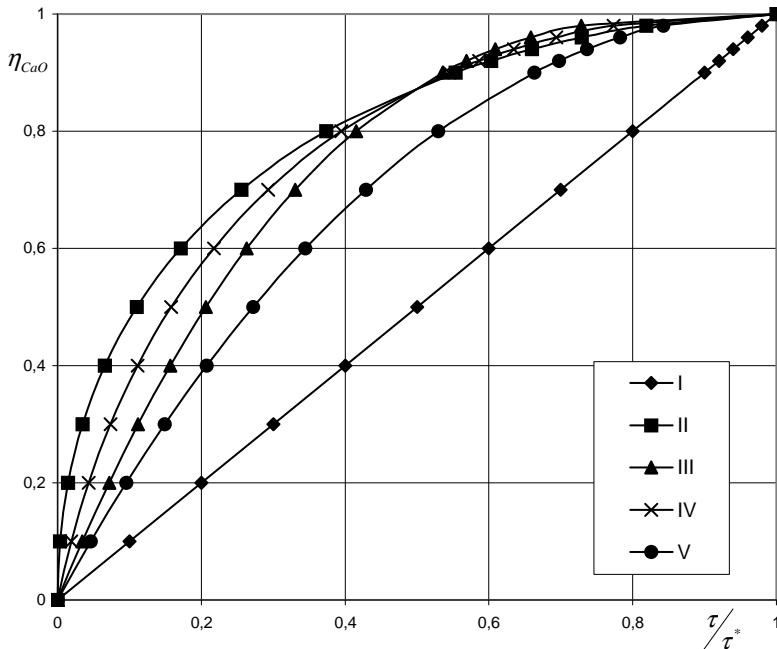


Figure 4. Conversion versus reduced time for different kinetic regimes (I, II, III, IV, V).

The most favorable kinetic regime is that providing the greatest conversion at a given time. It can be seen from Figure 4 that, to achieve conversions above 90%, the kinetic regime III, with no transfer limitation, is the most advantageous. Practically, the diffusion influence is not avoidable when a compact solid is formed.

Therefore, a regime of VI type may be frequently encountered in practice. This could be a rather effective regime when conversions under 90% would be accepted in practice.

The next paragraph is devoted to the estimation of the kinetic constants, on the basis of our own experimental data and the postulated unreacted core model, in order to evaluate the kinetic regime for a given set of operation factors: temperature, particle size, gas flow rate and composition.

### Kinetic coefficients identification

The kinetic coefficients characterizing the three individual steps of the process have been defined by the kinetic equations (5), (6), and (7). They are  $k_g$ ,  $D_s$ , and  $k$  respectively.

The mass transfer coefficient can be predicted quite accurately with the correlation proposed by Rantz and Marshall [21]:

$$Sh = 2.0 + 0.6 Re^{1/2} Sc^{1/3} \quad (17)$$

using experiments confined to the Reynolds number range 0 to 200. Froessling [22] had earlier presented an almost identical equation, and theoretically showed that the Sherwood number should take on a value of 2.0 in stagnant fluid. Froessling's experiments concerned the evaporation of nitrobenzene, aniline, water, and naphthalene into hot air stream. The Froessling – Rantz – Marshall equation (17) is still accepted as the most rigorous [23] in spite of the later extensive studies on the subject of mass transfer from solid spheres [24,25]. Therefore it has been used in previous papers on the lime – sulphur dioxide reaction [26-28].

The gas properties involved in the Sh, Re, and Sc numbers have been calculated for our experimental conditions. The molecular diffusivity of SO<sub>2</sub> has been evaluated with the equation proposed by Fuller et al. [29]. The results are presented in Table1:

**Table 1.**

#### **Gas properties and flow rates for the experimental conditions:**

$$P = 0.3403 \text{ bar}, A = 3.8 \cdot 10^{-4} \text{ m}^2, V_g = 50 \text{ cm}^3/\text{min}.$$

T, K	$V_g, 10^6 \text{ m}^3/\text{s}$	$v_g, \text{ m/s}$	$\rho_g, \text{ kg/m}^3$	$\mu_g, 10^5 \text{ Pa}\cdot\text{s}$	$D_{\text{SO}_2}, 10^4 \text{ m}^2/\text{s}$
973	8.7275	0.0230	0.123	4.086	2.930
1023	9.1760	0.0241	0.117	4.202	3.206
1123	10.0729	0.0265	0.106	4.434	3.775
1173	10.5213	0.0277	0.102	4.550	4.074

With the values from Table 1 introduced into the equation (17) the mass transfer coefficients in Table 2 have been obtained.

**Table2.****Mass transfer coefficients ( $k_g$ , m/s) at the experimental conditions.**P = 0.3403 bar,  $V_g = 50 \text{ cm}^3/\text{min}$ .

$d_p, \mu\text{m}$	25	90	180	450	900
973	23.7325	6.6653	3.3646	1.3711	0.6998
1023	25.9631	7.2905	3.6793	1.4912	0.7649
1123	30.5606	8.5789	4.3288	1.7627	0.8989
1173	32.9772	9.2563	4.6702	1.8298	0.9695

The value of  $k_g$  is more sensitive to the particle size variation than to the temperature change, as expected.

The reaction rate constant ( $k$ ) can be derived from the thermogravimetric data obtained with the smallest particles ( $R_0 = 12.5 \mu\text{m}$ ) at low conversions (<10%) when the diffusion influence may be supposed as negligible. This is the extreme case III, described by the equation (10) reduced to the form:

$$F(\eta) = 1 - (1 - \eta_{CaO})^{1/3} = \frac{kC_{SO_2}^0 \tau}{R_0 C_{CaO}^0} \quad (18)$$

By representing  $F(\eta)$  versus time, using the points from curves in Figure 2, the constant  $k$  can be calculated with the relation (19):

$$k = \frac{C_{CaO}^0 R_0}{C_{SO_2}} \left[ \frac{dF(\eta)}{d\tau} \right]_{T=const.} \quad (19)$$

Where:  $C_{CaO}^0 = 3370 \times 0.95 / 56 = 57.17 \text{ kmol/m}^3$ ;  $C_{SO_2} = 0.009/22.4 = 4.01785 \cdot 10^{-4} \text{ kmol/m}^3$ , and  $R_0 = 12.5 \cdot 10^{-6} \text{ m}$ .

The values of  $k$  identified in such a manner are listed in Table 5 (with \*superscript) together with those derived from Borgwardt 's data using the grain model [3,4] by Hartman and Trnka [13].

**Table 3.****Kinetic constants of the reaction of lime with sulfur dioxide**

T, K	k, $10^4 \text{ m/s}$		$D_e, 10^5 \text{ m}^2/\text{s}$	$D_s, 10^{12} \text{ m}^2/\text{s}$	$r_g, 10^7 \text{ m}$
973	3.16		-	-	-
1073	-	3.04	6.94	1.4	2.85
1123	3.75	4.95	7.50	5.5	3.74
1173	4.15	7.76	8.07	7.4	4.86

The values of  $k$  derived from our thermogravimetric data have the same order of magnitude with those calculated by Hartman and Trnka [13]. Nevertheless, there is a great difference regarding the activation energy: that from Borgwardt's data is 79.6 kJ/mol whereas our data lead to an activation energy smaller than 41.8 kJ/mol. This means that our  $k$  is only an apparent rate constant, the process being in the kinetic regime VI (reaction controlled by diffusion).

Another way to check the kinetic regime is suggested by the equation (11), which may be translated into the following words: the time for complete conversion

of a particle is the sum of complete reaction times corresponding to extreme cases I to III:

$$\tau^* = \sum_{i=I}^{i=III} \tau_i^* \quad (11')$$

Using the values of  $k_g$ ,  $k$ , and  $D_s$  from Tables 4 and 5 it is possible to evaluate the relative complete reaction times at given values of parameters: temperature, particle size, gas flow rate. With  $T = 1.123 \text{ K}$ ,  $R_0 = 12.5 \text{ } \mu\text{m}$ , and gas flow rate of  $50 \text{ cm}^3/\text{min}$ , the relative contributions of the three reaction steps are the following:

$$\left( \tau_I^* / \tau^* \right) \cdot 100 = 0.02449; \quad \left( \tau_{II}^* / \tau^* \right) \cdot 100 = 84.8503; \quad \left( \tau_{III}^* / \tau^* \right) \cdot 100 = 15.1252$$

In other words, even with the smallest particles, the process investigated was kinetically controlled by diffusion in a proportion of 85 %. The chemical reaction share was only 15 %, whereas the external mass transfer had no influence. Consequently, the industrial process could be enhanced mainly through the factors accelerating the solid phase diffusion.

### Conclusions and significance

The dry injection of limestone fine particles in the power plant furnaces is a promising process for flue gas desulphurization and acid rain mitigation. The limestone is quickly converted to lime which further reacts with sulphur dioxide. New kinetic studies have been carried out on the sulfation reaction using a CAHN TG –121 system for continuous thermogravimetric measurements. The kinetic curves are quantitatively analyzed on the basis of the unreacted core model integrated in the general form. This includes the three steps connected in series: external mass transfer, diffusion, and chemical reaction at the core surface. The corresponding kinetic coefficients are identified for the experimental operating conditions: temperature, particles size, gas composition and flow rate. The first practical conclusion is that, even with low gas rates used in the thermobalance (0.0230 to 0.0277 m/s) the external mass transfer has no influence on the overall rate of the process.

The second conclusion is that even with the smallest particles ( $d_p = 25 \text{ } \mu\text{m}$ ) and temperatures as low as 1123 K the internal diffusion "resistance" can not be avoided. Improved structured models and complementary experimental techniques are needed for a better understanding and quantitative description of the lime sulphation reaction in order to enhance the industrial process.

### Notations

- A – cross section area of the reactor,  $\text{m}^2$ ;
- A'' – inert substances in the solid, -;
- C – molar concentration,  $\text{kmol} / \text{m}^3$ ;
- $d_p$  – particle diameter, m;
- $D_e$  – effective diffusion coefficient,  $\text{m}^2 / \text{s}$ ;

- $D_S$  – diffusion coefficient in the product layer,  $m^2/s$ ;  
 $D_{SO_2}$  – molecular diffusion coefficient of  $SO_2$  in the gas mixture,  $m^2/s$ ;  
 $H$  – height of the reaction tube,  $m$ ;  
 $k$  – surface reaction rate constant,  $m/s$ ;  
 $k_g$  – mass transfer coefficient in the gas phase,  $m/s$ ;  
 $K$  – overall coefficient of the process, defined by equation (13),  $m/s$ ;  
 $m_i$  – mass of component,  $kg$ ;  
 $P$  – pressure,  $Pa$ ;  
 $r$  – radius of the grain unreacted core,  $m$ ;  
 $r_g$  – grain radius,  $m$ ;  
 $R$  – radius of the unreacted core of particle,  $m$ ;  
 $R_0$  – initial radius of the particle,  $m$ ;  
 $S$  – surface area of particle,  $m^2$ ;  
 $T$  – temperature,  $K$ ;  
 $v_g$  – gas rate,  $m/s$ ;  
 $V_g$  – gas flow rate,  $m^3/s$ ;  
 $x_{CaO}^0$  – mass fraction of  $CaO$  in the lime, –;  
 $\Delta m_s$  – thermogravimetric mass increase,  $kg$ ;  
 $\eta_{CaO}$  – fractional conversion of  $CaO$  in the reaction (2), –;  
 $\mu_g$  – gas viscosity,  $Pa \cdot s$ ;  
 $\rho_g$  – gas density,  $kg/m^3$ ;  
 $\rho_s$  – solid density,  $kg/m^3$ ;  
 $\tau$  – reaction time,  $s$ ;  
 $\tau^*$  – time for complete reaction,  $s$ ;

### Subscripts

- $c$  – related to calcination;  
 $ex$  – external surface of the particle;  
 $g$  – grain or gas phase;  
 $L$  – lime;  
 $LS$  – limestone;  
 $r$  – reaction;  
 $s$  – solid phase;

### Superscripts

- $0$  – initial state ( $\tau = 0$ );  
 $s$  – surface of the particle.

## REFERENCES

1. Bjerle, J., Ye, Z., Wang, W., *Limits and potentials of the dry injection process, 1993 SO<sub>2</sub> Control Symposium*, 1993 vol. 1, EPRI, Boston.
2. Dunderdale, J. (Editor), *Energy and the Environment*, Royal. Soc., 1990 Cambridge.
3. Borgwardt, R.H., *Environ. Sci. Technol.*, (1970) 4, 59.
4. Borgwardt, R.H., Harvey, R.D., *Environ. Sci. Technol.*, (1970) 6, 350.
5. Borgwardt, R.H., Roache, N.F., Bruce, K.R., *Environ. Prog.*, (1984) 3, 129.
6. Borgwardt, R.H., *A.I. Ch. E. Journal*, (1985) 31, 1, 103.
7. Borgwardt, R.H., Roache, N.F., Bruce, K.R., *Ind. Eng. Chem. Fundam.*, (1985) 25, 156.
8. Borgwardt, R.H., Bruce, K.R., Blake, J., *Ind. Eng. Chem. Res.*, (1987) 26, 1993.
9. Borgwardt, R.H., *Chem. Eng. Sci.*, (1989) 44, 1, 53.
10. Wen, C.Y., Ishida, M., *Environ. Sci. Technol.*, (1973) 7, 703.
11. Pigford, R.L., Sliger, G., *Ind. Eng. Chem. Process Des. Dev.*, (1973) 12, 85.
12. Hartman, M., Coughlin, W.R., *Ind. Eng. Chem. Process Des. Dev.*, (1974) 13, 248.
13. Hartman, M., Trnka, O., *Chem. Eng. Sci.*, (1980) 35, 1189.
14. Hartman, M., Svoboda, K., Trnka, O., *Sulfur dioxide removal in a batch fluidized bed reactor*, EFCE Publ. Series, (1984) No. 37, Pergamon Press, Oxford, 509.
15. Fields, R.B., Burdett, N.A., Davidson, J.F., *Trans. Instn. Chem. Engrs.*, (1979) 57, 276.
16. Hartman, M., *Colln. Czech Chem. Commun.*, (1975) 40, 1466.
17. Borgwardt, R.H., *2<sup>nd</sup> Joint Symposium on Dry SO<sub>2</sub> and Simultaneous SO<sub>2</sub>/NO<sub>x</sub> Control Technologies*, San Diego, California, 1984.
18. Yang, R.T., Cunningham, P.T., Wilson, W.I., Johnson, S.A., *Adv. Chem. Ser.*, (1975) 134, 149.
19. O'Neil, E.P., Kearns, D.L., Kittle, W.F., *Thermochim. Acta.*, (1976) 14, 209.
20. Bjerle, J., Xu, F., Ye, Z., *Chem. Eng. Technol.*, (1992) 15, 151.
21. Rantz, W.E., Marshall, W.R., *Chem. Eng. Prog.*, (1952) 48, 173.
22. Froessling, M., *Beitr. Geophys.*, (1938) 52, 170.
23. Froment, G.F., Bischoff, K.B., *Chemical Reactor Analysis and Design*, 2<sup>nd</sup> Edition Wiley, New York, 1990.
24. Hughmark, G.A., *A.I.Ch.E. Journal*, (1967) 13, 1219.
25. Levender, W.J., Pei, D.C.T., *Int. J. Mass Trans.*, (1967) 10, 529.
26. Alen, D., Hayhurst, A.N., *J.Chem.Soc. Faraday Trans.*, (1996) 92, 7, 1227.
27. Dennis, J.S., Hayhurst, A.N., *Chem. Eng. Sci.*, (1990) 45, 5, 1175.
28. Tambe, S., Gauri, K.L., Li, S., Coburn, W.G., *Environ.Sci. Technol.*, (1991) 25, 2071.
29. Fuller, E.N., Schettler, P.D., Giddings, J.C., *Ind.Eng. Chem.*, (1966) 58, 5, 19.
30. Georgakis, C., Chang, C.W., Szekely, J., *Chem.Eng.Sci.*, (1979) 34, 1072.
31. Sotirchos, S.V., Yu, H.C., *Chem.Eng.Sci.*, (1985) 40, 2039.
32. Adanez, J., Gayan, P., Garcia-Labiano, F., *Ind.Eng.Chem.Res.*, (1996) 35, 2190.
33. Fernandez, I., Garea, A., Irabien, A., *Chem.Eng.Sci.*, (1998) 53, 1869.